

Measurement of identified π^0 and inclusive photon v_2 and implication to the direct photon production in $\sqrt{s_{NN}} = 200$ GeV Au+Au collisions

S.S. Adler,⁵ S. Afanasiev,¹⁷ C. Aidala,⁵ N.N. Ajitanand,⁴³ Y. Akiba,^{20,38} J. Alexander,⁴³ R. Amirkas,¹² L. Aphecetche,⁴⁵ S.H. Aronson,⁵ R. Auerbeck,⁴⁴ T.C. Awes,³⁵ R. Azmoun,⁴⁴ V. Babintsev,¹⁵ A. Baldisseri,¹⁰ K.N. Barish,⁶ P.D. Barnes,²⁷ B. Bassalleck,³³ S. Bathe,³⁰ S. Batsouli,⁹ V. Baublis,³⁷ A. Bazilevsky,^{39,15} S. Belikov,^{16,15} Y. Berdnikov,⁴⁰ S. Bhagavatula,¹⁶ J.G. Boissevain,²⁷ H. Borel,¹⁰ S. Borenstein,²⁵ M.L. Brooks,²⁷ D.S. Brown,³⁴ N. Bruner,³³ D. Bucher,³⁰ H. Buesching,³⁰ V. Bumazhnov,¹⁵ G. Bunce,^{5,39} J.M. Burward-Hoy,^{26,44} S. Butsyk,⁴⁴ X. Camard,⁴⁵ J.-S. Chai,¹⁸ P. Chand,⁴ W.C. Chang,² S. Chernichenko,¹⁵ C.Y. Chi,⁹ J. Chiba,²⁰ M. Chiu,⁹ I.J. Choi,⁵² J. Choi,¹⁹ R.K. Choudhury,⁴ T. Chujo,⁵ V. Cianciolo,³⁵ Y. Cobigo,¹⁰ B.A. Cole,⁹ P. Constantin,¹⁶ D. d'Enterria,⁴⁵ G. David,⁵ H. Delagrangé,⁴⁵ A. Denisov,¹⁵ A. Deshpande,³⁹ E.J. Desmond,⁵ A. Devismes,⁴⁴ O. Dietzsch,⁴¹ O. Drapier,²⁵ A. Drees,⁴⁴ R. du Rietz,²⁹ A. Durum,¹⁵ D. Dutta,⁴ Y.V. Efremenko,³⁵ K. El Chenawi,⁴⁹ A. Enokizono,¹⁴ H. En'yo,^{38,39} S. Esumi,⁴⁸ L. Ewell,⁵ D.E. Fields,^{33,39} F. Fleuret,²⁵ S.L. Fokin,²³ B.D. Fox,³⁹ Z. Fraenkel,⁵¹ J.E. Frantz,⁹ A. Franz,⁵ A.D. Frawley,¹² S.-Y. Fung,⁶ S. Garpman,²⁹ * T.K. Ghosh,⁴⁹ A. Glenn,⁴⁶ G. Gogiberidze,⁴⁶ M. Gonin,²⁵ J. Gosset,¹⁰ Y. Goto,³⁹ R. Granier de Cassagnac,²⁵ N. Grau,¹⁶ S.V. Greene,⁴⁹ M. Grosse Perdekamp,³⁹ W. Guryn,⁵ H.-Å. Gustafsson,²⁹ T. Hachiya,¹⁴ J.S. Haggerty,⁵ H. Hamagaki,⁸ A.G. Hansen,²⁷ E.P. Hartouni,²⁶ M. Harvey,⁵ R. Hayano,⁸ N. Hayashi,³⁸ X. He,¹³ M. Heffner,²⁶ T.K. Hemmick,⁴⁴ J.M. Heuser,⁴⁴ M. Hibino,⁵⁰ J.C. Hill,¹⁶ W. Holzmann,⁴³ K. Homma,¹⁴ B. Hong,²² A. Hoover,³⁴ T. Ichihara,^{38,39} V.V. Ikonnikov,²³ K. Imai,^{24,38} D. Isenhower,¹ M. Ishihara,³⁸ M. Issah,⁴³ A. Isupov,¹⁷ B.V. Jacak,⁴⁴ W.Y. Jang,²² Y. Jeong,¹⁹ J. Jia,⁴⁴ O. Jinnouchi,³⁸ B.M. Johnson,⁵ S.C. Johnson,²⁶ K.S. Joo,³¹ D. Jouan,³⁶ S. Kametani,^{8,50} N. Kamihara,^{47,38} M. Kaneta,³⁹ J.H. Kang,⁵² S.S. Kapoor,⁴ K. Katou,⁵⁰ S. Kelly,⁹ B. Khachaturov,⁵¹ A. Khanzadeev,³⁷ J. Kikuchi,⁵⁰ D.H. Kim,³¹ D.J. Kim,⁵² D.W. Kim,¹⁹ E. Kim,⁴² G.-B. Kim,²⁵ H.J. Kim,⁵² E. Kistenev,⁵ A. Kiyomichi,⁴⁸ K. Kiyoyama,³² C. Klein-Boesing,³⁰ H. Kobayashi,^{38,39} L. Kochenda,³⁷ V. Kochetkov,¹⁵ D. Koehler,³³ T. Kohama,¹⁴ M. Kopytine,⁴⁴ D. Kotchetkov,⁶ A. Kozlov,⁵¹ P.J. Kroon,⁵ C.H. Kuberg,^{1,27} K. Kurita,³⁹ Y. Kuroki,⁴⁸ M.J. Kweon,²² Y. Kwon,⁵² G.S. Kyle,³⁴ R. Lacey,⁴³ V. Ladygin,¹⁷ J.G. Lajoie,¹⁶ A. Lebedev,^{16,23} S. Leckey,⁴⁴ D.M. Lee,²⁷ S. Lee,¹⁹ M.J. Leitch,²⁷ X.H. Li,⁶ H. Lim,⁴² A. Litvinenko,¹⁷ M.X. Liu,²⁷ Y. Liu,³⁶ C.F. Maguire,⁴⁹ Y.I. Makdisi,⁵ A. Malakhov,¹⁷ V.I. Manko,²³ Y. Mao,^{7,38} G. Martinez,⁴⁵ M.D. Marx,⁴⁴ H. Masui,⁴⁸ F. Matathias,⁴⁴ T. Matsumoto,^{8,50} P.L. McGaughey,²⁷ E. Melnikov,¹⁵ F. Messer,⁴⁴ Y. Miake,⁴⁸ J. Milan,⁴³ T.E. Miller,⁴⁹ A. Milov,^{44,51} S. Mioduszewski,⁵ R.E. Mischke,²⁷ G.C. Mishra,¹³ J.T. Mitchell,⁵ A.K. Mohanty,⁴ D.P. Morrison,⁵ J.M. Moss,²⁷ F. Mühlbacher,⁴⁴ D. Mukhopadhyay,⁵¹ M. Muniruzzaman,⁶ J. Murata,^{38,39} S. Nagamiya,²⁰ J.L. Nagle,⁹ T. Nakamura,¹⁴ B.K. Nandi,⁶ M. Nara,⁴⁸ J. Newby,⁴⁶ P. Nilsson,²⁹ A.S. Nyanin,²³ J. Nystrand,²⁹ E. O'Brien,⁵ C.A. Ogilvie,¹⁶ H. Ohnishi,^{5,38} I.D. Ojha,^{49,3} K. Okada,³⁸ M. Ono,⁴⁸ V. Onuchin,¹⁵ A. Oskarsson,²⁹ I. Otterlund,²⁹ K. Oyama,⁸ K. Ozawa,⁸ D. Pal,⁵¹ A.P.T. Palounek,²⁷ V. Pantuev,⁴⁴ V. Papavassiliou,³⁴ J. Park,⁴² A. Parmar,³³ S.F. Pate,³⁴ T. Peitzmann,³⁰ J.-C. Peng,²⁷ V. Peresedov,¹⁷ C. Pinkenburg,⁵ R.P. Pisani,⁵ F. Plasil,³⁵ M.L. Purschke,⁵ A.K. Purwar,⁴⁴ J. Rak,¹⁶ I. Ravinovich,⁵¹ K.F. Read,^{35,46} M. Reuter,⁴⁴ K. Reygers,³⁰ V. Riabov,^{37,40} Y. Riabov,³⁷ G. Roche,²⁸ A. Romana,²⁵ M. Rosati,¹⁶ P. Rosnet,²⁸ S.S. Ryu,⁵² M.E. Sadler,¹ N. Saito,^{38,39} T. Sakaguchi,^{8,50} M. Sakai,³² S. Sakai,⁴⁸ V. Samsonov,³⁷ L. Sanfratello,³³ R. Santo,³⁰ H.D. Sato,^{24,38} S. Sato,^{5,48} S. Sawada,²⁰ Y. Schutz,⁴⁵ V. Semenov,¹⁵ R. Seto,⁶ M.R. Shaw,^{1,27} T.K. Shea,⁵ T.-A. Shibata,^{47,38} K. Shigaki,^{14,20} T. Shiina,²⁷ C.L. Silva,⁴¹ D. Silvermyr,^{27,29} K.S. Sim,²² C.P. Singh,³ V. Singh,³ M. Sivertz,⁵ A. Soldatov,¹⁵ R.A. Soltz,²⁶ W.E. Sondheim,²⁷ S.P. Sorensen,⁴⁶ I.V. Sourikova,⁵ F. Staley,¹⁰ P.W. Stankus,³⁵ E. Stenlund,²⁹ M. Stepanov,³⁴ A. Ster,²¹ S.P. Stoll,⁵ T. Sugitate,¹⁴ J.P. Sullivan,²⁷ E.M. Takagui,⁴¹ A. Taketani,^{38,39} M. Tamai,⁵⁰ K.H. Tanaka,²⁰ Y. Tanaka,³² K. Tanida,³⁸ M.J. Tannenbaum,⁵ P. Tarján,¹¹ J.D. Tepe,^{1,27} T.L. Thomas,³³ J. Tojo,^{24,38} H. Torii,^{24,38} R.S. Towell,¹ I. Tseruya,⁵¹ H. Tsuruoka,⁴⁸ S.K. Tuli,³ H. Tydesjö,²⁹ N. Tyurin,¹⁵ H.W. van Hecke,²⁷ J. Velkovska,^{5,44} M. Velkovsky,⁴⁴ V. Veszprémi,¹¹ L. Villatte,⁴⁶ A.A. Vinogradov,²³ M.A. Volkov,²³ E. Vznuzdaev,³⁷ X.R. Wang,¹³ Y. Watanabe,^{38,39} S.N. White,⁵ F.K. Wohn,¹⁶ C.L. Woody,⁵ W. Xie,⁶ Y. Yang,⁷ A. Yanovich,¹⁵ S. Yokkaichi,^{38,39} G.R. Young,³⁵ I.E. Yushmanov,²³ W.A. Zajc,^{9,†} C. Zhang,⁹ S. Zhou,⁷ S.J. Zhou,⁵¹ and L. Zolin¹⁷

(PHENIX Collaboration)

¹Abilene Christian University, Abilene, TX 79699, USA

²Institute of Physics, Academia Sinica, Taipei 11529, Taiwan

³Department of Physics, Banaras Hindu University, Varanasi 221005, India

⁴Bhabha Atomic Research Centre, Bombay 400 085, India

- ⁵Brookhaven National Laboratory, Upton, NY 11973-5000, USA
⁶University of California - Riverside, Riverside, CA 92521, USA
⁷China Institute of Atomic Energy (CIAE), Beijing, People's Republic of China
⁸Center for Nuclear Study, Graduate School of Science, University of Tokyo, 7-3-1 Hongo, Bunkyo, Tokyo 113-0033, Japan
⁹Columbia University, New York, NY 10027 and Nevis Laboratories, Irvington, NY 10533, USA
¹⁰Dapnia, CEA Saclay, F-91191, Gif-sur-Yvette, France
¹¹Debrecen University, H-4010 Debrecen, Egyetem tér 1, Hungary
¹²Florida State University, Tallahassee, FL 32306, USA
¹³Georgia State University, Atlanta, GA 30303, USA
¹⁴Hiroshima University, Kagamiyama, Higashi-Hiroshima 739-8526, Japan
¹⁵IHEP Protvino, State Research Center of Russian Federation, Institute for High Energy Physics, Protvino, 142281, Russia
¹⁶Iowa State University, Ames, IA 50011, USA
¹⁷Joint Institute for Nuclear Research, 141980 Dubna, Moscow Region, Russia
¹⁸KAERI, Cyclotron Application Laboratory, Seoul, South Korea
¹⁹Kangnung National University, Kangnung 210-702, South Korea
²⁰KEK, High Energy Accelerator Research Organization, Tsukuba, Ibaraki 305-0801, Japan
²¹KFKI Research Institute for Particle and Nuclear Physics of the Hungarian Academy of Sciences (MTA KFKI RMKI), H-1525 Budapest 114, POBox 49, Budapest, Hungary
²²Korea University, Seoul, 136-701, Korea
²³Russian Research Center "Kurchatov Institute", Moscow, Russia
²⁴Kyoto University, Kyoto 606-8502, Japan
²⁵Laboratoire Leprince-Ringuet, Ecole Polytechnique, CNRS-IN2P3, Route de Saclay, F-91128, Palaiseau, France
²⁶Lawrence Livermore National Laboratory, Livermore, CA 94550, USA
²⁷Los Alamos National Laboratory, Los Alamos, NM 87545, USA
²⁸LPC, Université Blaise Pascal, CNRS-IN2P3, Clermont-Fd, 63177 Aubiere Cedex, France
²⁹Department of Physics, Lund University, Box 118, SE-221 00 Lund, Sweden
³⁰Institut für Kernphysik, University of Muenster, D-48149 Muenster, Germany
³¹Myongji University, Yongin, Kyonggido 449-728, Korea
³²Nagasaki Institute of Applied Science, Nagasaki-shi, Nagasaki 851-0193, Japan
³³University of New Mexico, Albuquerque, NM 87131, USA
³⁴New Mexico State University, Las Cruces, NM 88003, USA
³⁵Oak Ridge National Laboratory, Oak Ridge, TN 37831, USA
³⁶IPN-Orsay, Université Paris Sud, CNRS-IN2P3, BP1, F-91406, Orsay, France
³⁷PNPI, Petersburg Nuclear Physics Institute, Gatchina, Leningrad region, 188300, Russia
³⁸RIKEN, The Institute of Physical and Chemical Research, Wako, Saitama 351-0198, Japan
³⁹RIKEN BNL Research Center, Brookhaven National Laboratory, Upton, NY 11973-5000, USA
⁴⁰Saint Petersburg State Polytechnic University, St. Petersburg, Russia
⁴¹Universidade de São Paulo, Instituto de Física, Caixa Postal 66318, São Paulo CEP05315-970, Brazil
⁴²System Electronics Laboratory, Seoul National University, Seoul, South Korea
⁴³Chemistry Department, Stony Brook University, SUNY, Stony Brook, NY 11794-3400, USA
⁴⁴Department of Physics and Astronomy, Stony Brook University, SUNY, Stony Brook, NY 11794, USA
⁴⁵SUBATECH (Ecole des Mines de Nantes, CNRS-IN2P3, Université de Nantes) BP 20722 - 44307, Nantes, France
⁴⁶University of Tennessee, Knoxville, TN 37996, USA
⁴⁷Department of Physics, Tokyo Institute of Technology, Tokyo, 152-8551, Japan
⁴⁸Institute of Physics, University of Tsukuba, Tsukuba, Ibaraki 305, Japan
⁴⁹Vanderbilt University, Nashville, TN 37235, USA
⁵⁰Waseda University, Advanced Research Institute for Science and Engineering, 17 Kikui-cho, Shinjuku-ku, Tokyo 162-0044, Japan
⁵¹Weizmann Institute, Rehovot 76100, Israel
⁵²Yonsei University, IPAP, Seoul 120-749, Korea

(Dated: May 9, 2019)

The azimuthal distribution of identified π^0 and inclusive photons has been measured in $\sqrt{s_{NN}} = 200$ GeV Au+Au collisions with the PHENIX experiment at the Relativistic Heavy Ion Collider (RHIC). The second harmonic parameter (v_2) was measured to describe the observed anisotropy of the azimuthal distribution. The measured inclusive photon v_2 is consistent with the value expected for the photons from hadron decay and is also consistent with the lack of direct photon signal over the measured p_T range 1-6 GeV/c. An attempt is made to extract v_2 of direct photons.

PACS numbers: 25.75.Dw

Among the most exciting features of the experimental data from the Relativistic Heavy-Ion Collider (RHIC) are

the suppression of high p_T hadron yields [1, 2, 3, 4, 5], the baryon excess at intermediate p_T [6, 7, 8, 9], and

the quark number scaling of the identified hadron v_2 [10, 11]. Theoretically, the observed high p_T suppression has been attributed to energy loss of the hard-scattered partons [12, 13]. Experimentally, the absence of the suppression in d+Au collisions has shown that it is a final-state effect due to the hot and dense matter created in central Au+Au collisions [14, 15, 16, 17]. The quark number scaling of the measured elliptic flow parameter v_2 and the nuclear modification factor R_{cp} of baryons versus mesons may suggest the existence of a thermalized partonic phase before hadronization [18, 19].

The second harmonic coefficient parameter v_2 of the azimuthal distribution of the particles produced in heavy-ion collisions is defined by

$$\frac{dN}{d\phi} \propto 1 + 2 v_2 \cos(2(\phi - \Phi_{RP})), \quad (1)$$

where ϕ is the azimuthal direction of the particle and Φ_{RP} is the direction of the nuclear impact parameter (reaction plane) in a given collision. The v_2 in high-energy heavy-ion collisions is considered to be sensitive to the initial geometric overlap of the colliding nuclei as well as the later expansion driven by the initial pressure. Theoretically, the dominant source of v_2 at low p_T is the expansion of the dense matter in the direction of the short axis of the overlap zone, and at high p_T is the parton energy loss given by the shape of the geometrical overlap. The quark coalescence (recombination) might be responsible for the v_2 in the intermediate p_T region. However, the experimental definition of v_2 includes any 2nd harmonic correlation with respect to the event plane, which is given by the beam direction and the impact parameter direction. Detailed v_2 measurements of identified particles at higher p_T than 2 GeV/c, where hydro-dynamics alone does not describe the measurements, would enable us to understand the different mechanisms that generate v_2 and to investigate the transition region from low to high p_T . Especially, the v_2 of identified π^0 will give a baseline measurement of inclusive photon v_2 to extract the direct photon v_2 .

The direct photons produced in hard scattering are penetrating probes of the produced dense matter in heavy-ion collisions. Recently, we observed that the centrality dependence of the direct photon yield in $\sqrt{s_{NN}} = 200$ GeV Au+Au collisions is consistent with binary collision scaling [20]. The lack of suppression of direct photons is further evidence in favor of the final-state effect in hadron suppression. In addition to the initially-produced hard photons that should inherently follow binary scaling, there may be other counteracting effects resulting in apparent binary scaling. For example, some fraction of the photons may originate from partons having experienced energy loss, causing an analogous suppression of these photons [21] similar to hadrons. On the other hand, the parton energy loss may enhance the photon yield via Bremsstrahlung while passing through the hot and dense

matter [22]. The thermal emission of photons radiated from the hot and dense matter is also expected to increase direct photon yield for central Au+Au collisions [24].

The v_2 measurement of the direct photons could help to confirm that the observed binary scaling of the direct photon excess is attributable to the direct photon production being dominated by the initial hard scattering. The v_2 measurement of the direct photons would give additional and complementary information to help disentangle the various scenarios of direct photon production, as well as to provide more information on the dynamics and properties of the produced hot and dense matter. The v_2 of photons from the initial Compton-like hard scattering is expected to be zero if they do not interact with the hot and dense matter produced during the collision. However when the v_2 of high p_T hadrons is given purely by the parton energy loss, the photons from the parton fragmentation outside of the reaction zone should have v_2 similar to the hadrons at high p_T . Such photon fraction is expected to be about 50% of total direct photon yield at 3.5 GeV/c in p_T [21, 22]. On the other hand, one would expect that the photons originating from Bremsstrahlung due to the passage of partons through the hot and dense matter should have the opposite (negative) sign in v_2 compared with hadrons, because the parton energy loss is larger in the long axis of the overlapping region (out-of-plane). Finally, the photons from the thermal radiation should reflect the dynamical evolution of the produced hot and dense matter. There are recent theoretical predictions for different mechanisms [23].

In this letter we present measurements of the v_2 of π^0 and inclusive γ , as a function of transverse momentum and collision centrality, and we discuss the implications for the yield and v_2 of direct photons. The data are for 200 GeV Au+Au collisions from the PHENIX experiment [25] recorded during Run-2 (2001) at RHIC. The event trigger and centrality definition are given by the Beam-Beam Counters (BBC) and the Zero Degree Calorimeters (ZDC). The number of charged particles measured with the BBCs and the neutral spectators measured with the ZDCs are correlated with the number of participating nucleons, thus together providing a measure of the centrality. The event plane, which is a measure of reaction plane, is determined using the two BBCs at $|\eta| = 3.1 \sim 3.9$, where each counter consists of 64 photomultiplier tubes (PMT's) with quartz Cherenkov radiators in front, surrounding the beam pipe. The elliptic axis of the event plane Φ_{measured} is calculated by the angle weighted with the PMT amplitude using the second harmonic moment as described in refs.[10, 26]. The measured event anisotropy is corrected for a finite resolution of the measured event plane. The estimated event plane resolution $\sigma_{RP} = \langle \cos(2(\Phi_{\text{measured}} - \Phi_{RP})) \rangle$ is 0.3 on average, with a maximum of ~ 0.4 in the mid-central collisions. The corrected v_2 is calculated via the formula, $v_2 = \langle \cos(2(\phi - \Phi_{\text{measured}})) \rangle / \sigma_{RP}$. The phase space used

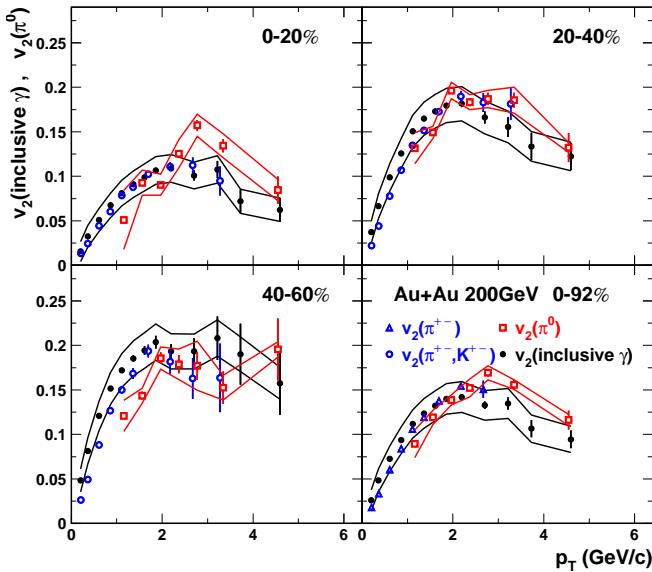


FIG. 1: (Color online) The measured v_2 of inclusive photon ($v_2^{\text{inclusive } \gamma}$, solid circle) and v_2 of π^0 ($v_2^{\pi^0}$, open square) for 4 centrality selections. The statistical (vertical error bars) and systematic errors (lines) are plotted separately. The highest p_T point corresponds to 4-6 GeV/c. Charged pion data are from previous measurements [10].

for the determination of the event plane for this analysis is 3 \sim 4 units away from the mid-rapidity, while the inclusive photon and the identified π^0 are measured at $|\eta| < 0.35$.

The photon identification and the π^0 reconstruction are performed in the same way as presented elsewhere [4]. The photon candidate clusters for both inclusive photon and π^0 measurement are first selected by their times-of-flight and the corresponding shower profiles in the electromagnetic calorimeter (EMCal). Neutral pions are reconstructed via $\pi^0 \rightarrow \gamma\gamma$ decay channel with an invariant mass analysis of γ pairs. An additional energy asymmetry cut, $|E_{\gamma 1} - E_{\gamma 2}| / (E_{\gamma 1} + E_{\gamma 2}) < 0.8$ is applied to the pairs of photon candidates in the π^0 reconstruction. The combinatorial background is estimated and subtracted by mixing pairs from different events with similar centrality, z-vertex position, and event plane orientation. The background is normalized in a region outside the π^0 mass peak for each bin in relative angle with respect to the measured event plane direction. A typical signal over background ratio is about 1 to 1 at $p_T = 3$ GeV/c in mid-central collisions (20-40% centrality). The v_2 of π^0 is calculated from the azimuthal distribution after the combinatorial background is subtracted for each centrality and p_T bin. For the inclusive photon analysis, the charged particle contamination in the sample of the photon candidate cluster is identified by associating the photon candidates with charged particle hits in the pad chamber (PC3) directly in front of the EMCal. The frac-

tion of photon candidates removed by this charge veto cut is about 15-25% depending on centrality. The effect of hadron contamination on the measured v_2 of inclusive photons is estimated by varying the size of the charged particle association window in the PC3, and no significant effect is seen. Neutron and anti-neutron contamination and off-vertex photons in the identified photon sample are studied with full detector Monte-Carlo simulation. The correction for these effects is applied to the data; it is 2% relative to the measured v_2 at 2 GeV/c and negligible at 4 GeV/c. The systematic error includes the effects from the π^0 and photon identification cuts and from the event plane determination: 5% for π^0 and 5% for photon identification and 5-10% for event plane determination given by the error on the correction factor from the finite event plane resolution. The analysis includes both a minimum-bias sample (30M events) and a Level2 trigger sample (equivalent to 55M events), where the Level2 algorithm is described in [20].

Figure 1 shows the measured v_2 of π^0 and inclusive photons as a function of p_T for different centrality selections. Data are compared with previous measurements of charged pions [10]. The p_T and centrality dependences of both the π^0 and the inclusive photon v_2 is consistent with that of other mesons [10]. The v_2 values are significantly above zero up to the highest p_T points. The non-zero v_2 of π^0 up to the highest p_T cannot be explained by flow effects alone, but may be attributed to jet quenching and/or quark coalescence (recombination).

Figure 2 compares for different centralities the v_2 of inclusive photons with the expected photon v_2 from hadronic decays. The expected photon v_2 from hadronic decays ($v_2^{b.g.}$) is calculated by Monte Carlo simulation with the measured v_2 of π^0 and other hadronic sources of photon. The relative yield of other sources (mainly η) is about 20% of the total hadronic decay photons, which corresponds to about 4% relative contribution in v_2 at 1 GeV/c and negligible at 3 GeV/c. In the simulation, we assume that the v_2 of η is similar to the kaon (the closest in mass particle) v_2 measured in [10, 11].

The v_2 of the inclusive photons $v_2^{\text{inclusive } \gamma}$ can be expressed as,

$$v_2^{\text{inclusive } \gamma} = \frac{v_2^{\text{direct } \gamma} N_{\text{direct } \gamma} + v_2^{b.g.} N_{b.g.}}{N_{\text{direct } \gamma} + N_{b.g.}}, \quad (2)$$

where $v_2^{\text{direct } \gamma}$ is the direct photon v_2 , $N_{\text{direct } \gamma}$ is the direct photon yield, and $N_{b.g.}$ is the background photon yield. Using the direct photon excess ratio $R = (N_{\text{direct } \gamma} + N_{b.g.}) / N_{b.g.}$, previously measured in [20], one can express the direct photon v_2 as:

$$v_2^{\text{direct } \gamma} = \frac{R v_2^{\text{inclusive } \gamma} - v_2^{b.g.}}{R - 1}. \quad (3)$$

The bottom data points in each panel of Fig. 2 show the difference: $R v_2^{\text{inclusive } \gamma} - v_2^{b.g.}$ (the numerator in

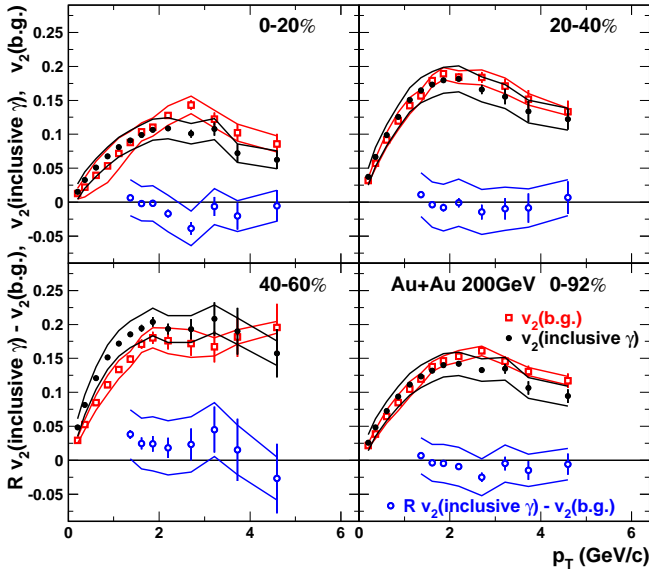


FIG. 2: (Color online) The measured v_2 of inclusive photons ($v_2^{inclusive \gamma}$, solid circle) and expected photon v_2 from hadronic decay ($v_2^{b.g.}$, open square). A subtracted v_2 quantity $Rv_2^{inclusive \gamma} - v_2^{b.g.}$ is plotted at the bottom of each panel (open circle), where $R = (N_{direct \gamma} + N_{b.g.})/N_{b.g.}$. The quantity corresponds to a product of the direct photon v_2 and a positive factor $R - 1$, ($v_2^{direct \gamma}(R - 1)$).

the above equation), which corresponds to a product of the direct photon v_2 times a positive factor $R - 1$, $v_2^{direct \gamma}(R - 1)$. Alternatively, it would be possible to calculate $v_2^{direct \gamma}$ using the measured ratio R [20]. However, we have chosen this subtracted quantity in order to show the direct photon v_2 and its sign, because $R - 1$ is measured to be small, especially at low p_T , and is sometimes negative experimentally. The comparison between $v_2^{inclusive \gamma}$ and $v_2^{b.g.}$ in each panel indicates that the measured inclusive photon v_2 is consistent with the expected photon v_2 from hadronic decay over the measured p_T range. The subtracted points are close to zero, which is also expected because of the lack of the direct photon signal in the measured p_T range, where R is close to unity [20]. The subtraction is especially meaningful where the measured R value goes above 1.0 at about 4-6 GeV/ c and higher p_T in central Au+Au collisions [20]; a region where one could extract the direct photon v_2 . The measurement indicates that v_2 of the direct photon is small at least in the highest p_T (4-6 GeV/ c) range in central Au+Au collisions. However, some hidden important trends (slightly negative or positive v_2 of direct photon) as a function of p_T and centrality could be extracted, once the errors on those two v_2 's and on the measured R are small enough. This is because the plotted subtracted quantity needs to be magnified by $1/(R - 1)$ in order to get the direct photon v_2 . The extracted direct photon v_2 at 4-6 GeV/ c is -1.5% with $\pm 6.4\%$ statistical and

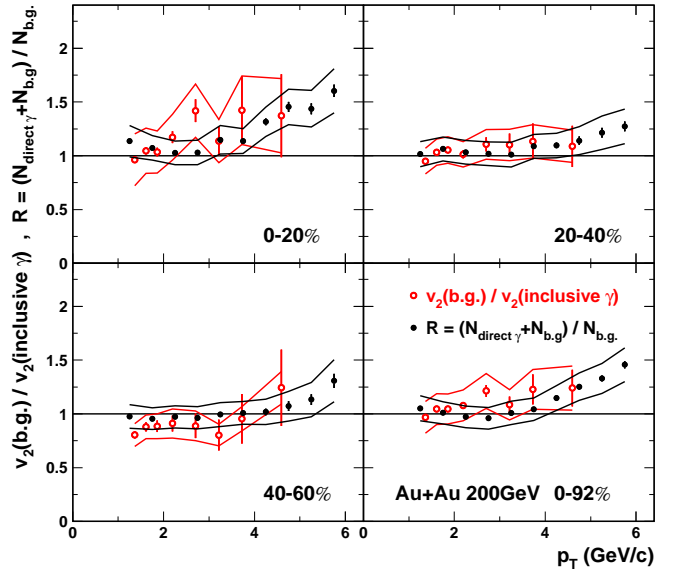


FIG. 3: (Color online) The ratio of the hadronic decay photon v_2 over inclusive photon v_2 ($v_2^{b.g.}/v_2^{inclusive \gamma}$, open circle) compared with the direct photon excess ratio $R = (N_{direct \gamma} + N_{b.g.})/N_{b.g.}$, (solid circle).

$\pm 6.4\%$ systematic errors for 0-20% central events and $-2.4\% \pm 6.7\%$ (sta.) $\pm 9.8\%$ (sys.) for 0-92% (minimum bias) events.

Figure 3 shows the ratio of $v_2^{b.g.}/v_2^{inclusive \gamma}$ and a comparison to the measured ratio R of the yields from [20]. If the direct photon v_2 is assumed to be zero, the ratio R should be equal to $v_2^{b.g.}/v_2^{inclusive \gamma}$ according to the Eq. 3. If the measured direct photon excess comes from the initial hard scattering, that would correspond to zero $v_2^{direct \gamma}$, then the measured v_2 ratio $v_2^{b.g.}/v_2^{inclusive \gamma}$ gives a consistent check of the direct photon excess ratio R measurement, especially where R is significantly above 1.0. The measured v_2 ratio as a function of p_T and centrality is consistent with the conventional relative yield measurement of the direct photon excess ratio R , but has somewhat larger errors.

In conclusion, the v_2 of identified π^0 and inclusive photons as a function of p_T and centrality are measured with the PHENIX central arm spectrometer at $|\eta| < 0.35$ with respect to the event plane defined at $|\eta| = 3.1 \sim 3.9$ in 200 GeV Au+Au collisions at RHIC. The v_2 of identified π^0 shows a similar trend as a function of p_T and centrality compared with other mesons and has values significantly above zero up to the highest p_T point. The measured v_2 of the inclusive photons is consistent with the v_2 of photons from hadronic decays, which is furthermore consistent with the absence of direct photon signal over the measured p_T range. However, the measurement indicates a small direct photon v_2 for the highest p_T (4-6 GeV/ c) range in central Au+Au collisions. The ratio of the estimated photon v_2 from the hadronic decay over

the measured inclusive photon v_2 is also consistent with the direct photon excess ratio measured via conventional yields ratio. This should also imply that the v_2 of direct photons is zero where the measured direct photon excess ratio R is significantly above 1.0. The present statistics and systematic accuracy of the data from the second year of RHIC running do not allow us to explicitly state the magnitude of direct photon v_2 . However, the indication of small v_2 for direct photons would favor the naive scenario of direct photon production from initial hard scattering and its small interaction with produced matter in high energy Au+Au collisions.

We thank the staff of the Collider-Accelerator and Physics Departments at BNL for their vital contributions. We acknowledge support from the Department of Energy and NSF (U.S.A.), MEXT and JSPS (Japan), CNPq and FAPESP (Brazil), NSFC (China), CNRS-IN2P3 and CEA (France), BMBF, DAAD, and AvH (Germany), OTKA (Hungary), DAE and DST (India), ISF (Israel), KRF and CHEP (Korea), RMIST, RAS, and RMAE (Russia), VR and KAW (Sweden), U.S. CRDF for the FSU, US-Hungarian NSF-OTKA-MTA, and US-Israel BSF.

* Deceased

† PHENIX Spokesperson:zajc@nevis.columbia.edu

[1] K. Adcox *et al.*, Phys. Rev. Lett. **88**, 022301 (2002).

- [2] C. Adler *et al.*, Phys. Rev. Lett. **89**, 212301 (2002).
 [3] K. Adcox *et al.*, Phys. Lett. **B561**, 82 (2003).
 [4] S. S. Adler *et al.*, Phys. Rev. Lett. **91**, 072301 (2003).
 [5] S. S. Adler *et al.*, Phys. Rev. **C69**, 034910 (2004).
 [6] S. S. Adler *et al.*, Phys. Rev. Lett. **91**, 172301 (2003).
 [7] S. S. Adler *et al.*, Phys. Rev. **C69**, 034909 (2004).
 [8] K. Adcox *et al.*, Phys. Rev. **C69**, 024904 (2004).
 [9] S. S. Adler *et al.*, nucl-ex/0410012 (2004).
 [10] S. S. Adler *et al.*, Phys. Rev. Lett. **91**, 182301 (2003).
 [11] J. Adams *et al.*, Phys. Rev. Lett. **92**, 052302 (2004).
 [12] X.-N. Wang, Phys. Lett. **B579**, 299 (2004).
 [13] M. Gyulassy, P. Levai and I. Vitev, Phys. Lett. **B538**, 282 (2002).
 [14] S. S. Adler *et al.*, Phys. Rev. Lett. **91**, 072303 (2003).
 [15] J. Adams *et al.*, Phys. Rev. Lett. **91**, 072304 (2003).
 [16] B. B. Back *et al.*, Phys. Rev. Lett. **91**, 072302 (2003).
 [17] I. Arsene *et al.*, Phys. Rev. Lett. **91**, 072305 (2003).
 [18] R. J. Fries, B. Müller, C. Nonaka and S. A. Bass, Phys. Rev. **C68**, 044902 (2003).
 [19] V. Greco, C. M. Ko and P. Levai, Phys. Rev. **C68**, 034904 (2003).
 [20] S. S. Adler *et al.*, Phys. Rev. Lett. **94**, 232301 (2005).
 [21] B. G. Zakharov, JETP Lett. **80**, 1 (2004).
 [22] R. J. Fries, B. Müller and D. K. Srivastava, Phys. Rev. Lett. **90**, 132301 (2003).
 [23] S. Turbide, C. Gale, R. J. Fries, hep-ph/0508201.
 [24] E.L. Feinberg, Nuovo Cimento **34**, 391 (1976); E.V. Shuryak, Phys. Lett. **B78**, 150 (1978); S. Turbide, R. Rapp, C. Gale, Phys. Rev. **C69**, 014903 (2004).
 [25] K. Adcox *et al.*, Nucl. Instrum. Methods **A499**, 469 (2003).
 [26] A. M. Poskanzer and S. A. Voloshin, Phys. Rev. **C58**, 1671 (1998).